Comparison of the EGFR resistance mutation profiles generated by EGFR targeted tyrosine kinase inhibitors and the impact of drug combinations

Egle Avizienyte[†], Richard A. Ward and Andrew P. Garner*

*Corresponding author

Andy.Garner@astrazeneca.com

AstraZeneca

Cancer & Infection Research Area

Macclesfield, SK10 4TG

UK.

[†]Current address: Translational Anti-Angiogenesis Laboratory, School of Cancer and Imaging Sciences, The University of Manchester, Wilmslow Road, Manchester, M20 4BX

Running title: Comparison of EGFR resistance mutation spectra

Key words: Resistance, ErbB2, EGFR, lapatinib, erlotinib, CI-1033

Manuscript length: 22 text pages, 4 tables and 5 figures

Supplementary data: 5 figures

Abstract length: 200 words

Word count (excluding references and figure legends): 5435

Abstract

Recent clinical data indicates that the emergence of mutant drug-resistant kinase alleles may be particularly relevant for targeted kinase inhibitors. In order to explore the how different classes of targeted therapies impact upon resistance mutations we performed EGFR resistance mutation screens with erlotinib, lapatinib and CI-1033. Distinct mutation spectra were generated with each inhibitor and were reflective of their respective mechanisms of action. Lapatinib yielded the widest variety of mutations, whilst mutational variability was lower in the erlotinib and CI-1033 screens. Lapatinib was uniquely sensitive to mutations of residues located deep within the selectivity pocket, whilst mutation of either G796 or C797 resulted in a dramatic loss of CI-1033 potency. The clinically observed T790M mutation was common to all inhibitors but occurred with varying frequencies. Importantly, the presence of C797S with T790M in the same EGFR allele conferred complete resistance to erlotinib, lapatinib and CI-1033. Combination of erlotinib and CI-1033 effectively reduced the number of drug resistant clones suggesting a possible clinical strategy to overcome drug resistance. Interestingly, our data also indicates that co-expression of ErbB2 has an impact upon the EGFR resistance mutations obtained suggesting that ErbB2 may play an active role in the acquisition of drug resistant mutations.

Introduction

Clinical data has indicated that the use of targeted therapies to selectively inactivate an oncogenic kinase creates selective pressures that a tumour can overcome through the outgrowth of a drug resistant population [1]. Mutations that confer resistance to targeted therapies have emerged as one of the common mechanisms for acquired secondary resistance [2,3]. For example, BCR-Abl mutations are speculated to be responsible for 50-90% of chronic myeloid leukaemia relapses following imatinib treatment [2]. A similar mechanism of resistance through mutation can also occur in non-small cell lung cancer (NSCLC) patients treated with EGFR inhibitors [3]. Approximately 50% of relapsed patients acquire a gatekeeper mutation (T790M) within the EGFR kinase domain [3] that is structurally analogous to the T315I mutation commonly found in BCR-Abl. Thus far, gatekeeper mutants have proved particularly difficult to overcome in the clinic presumably because many kinase inhibitors are designed to interact with the adjacent hydrophobic (selectivity) pocket. Interestingly, a family of irreversible inhibitors that form a covalent bond with residue C797 within the EGFR kinase domain demonstrate significant preclinical potency versus EGFR T790M [4-6]. Consequently, examples of irreversible inhibitors such as EKB-569 [7] and HKI-272 [8] are now being evaluated in relapsed NSCLC patients.

Since resistance mutations appear to be a recurring clinical issue we were particularly interested in exploring the structural relationships between kinase inhibitors and the point mutations that confer resistance to them. We chose to examine EGFR as a model system since there are multiple types of EGFR inhibitors available with distinct mechanisms of action. Erlotinib (Figure 1) is a specific EGFR inhibitor that blocks activity through direct competition with ATP [9]. Lapatinib (Figure 1) is a dual inhibitor of EGFR and ErbB2 that binds in the ATP site. The crystal structure of lapatinib bound to EGFR revealed that it preferentially targets an inactive conformation of EGFR [10]. CI-1033 (PD 183805) (Figure 1) is a pan-ErbB family inhibitor that forms a covalent bond with EGFR C797 resulting in dramatically increased inhibitor potency [11]. Erlotinib, lapatinib and CI-1033 are of further interest, since they represent the three classes of inhibitors used to target ErbB family members in the clinic [12-14].

To compare the mutation spectra obtained we performed *in vitro* resistance screens and identified a variety of novel EGFR resistance mutations. We confirmed that T790M was particularly important for erlotinib resistance, whilst the pattern of resistance obtained with lapatinib was reminiscent of that obtained with imatinib [15] highlighting their similar conformational requirements. We also report that the potency of irreversible kinase inhibitors is significantly affected by mutation of residues involved in covalent attachment and that the presence of ErbB2 can influence the EGFR mutation spectrum induced by erlotinib. Finally, we combined two mutations to produce a form of EGFR that was completely insensitive to erlotinib, lapatinib and CI-1033 suggesting that this double mutant may be particularly difficult to treat if it arises in the clinic.

Materials and Methods

Cell Culture and Generation of Cell Lines.

Ba/F3 cells were cultured in RPMI-1640 medium (Sigma-Aldrich) supplemented with L-glutamine (2 mM), 10% (v/v) fetal calf serum and 0.1% (v/v) WEHI-3B conditioned medium as a source of IL-3. Ba/F3 cells expressing myc-tagged versions of EGFR, EGFR-L858R, ErbB2, and EGFR or EGFR-L858R

resistance mutants were generated by retroviral infection. Viruses were produced using the Phoenix packaging cell line. 1 x10^6 Ba/F3 cells were infected in the presence of 1.5 % WEHI-3B conditioned medium and 8 μg/ml polybrene (Sigma-Aldrich). Infections were carried out at 1400*g* for 45 minutes at 33ºC followed by overnight incubation at 37ºC. Cells expressing EGFR and ErbB2 proteins were selected in either 0.7 μg/ml puromycin (Sigma-Aldrich) or 300 μg/ml hygromycin (Invitrogen). When required, cells were switched to IL-3-free RPMI medium supplemented with either 20 ng/ml EGF (R&D Systems) or 10 ng/ml heregulin (R&D Systems). To generate Ba/F3 cells co-expressing EGFR and ErbB2, Ba/F3/ErbB2 cells were maintained in IL-3-free medium supplemented with 10 ng/ml heregulin. Cells were infected with EGFR-pBabe Puro and selected with 0.7 μg/ml puromycin and 300 μg/ml hygromycin.

Vector generation

EGFR-myc and ErbB2-myc were amplified from EGFR-myc-pENTRY or ErbB2-myc-pENTRY plasmids (kindly supplied by Dr D. Robinson, AstraZeneca, UK) using PfuUltra Hotstart PCR Master Mix (Stratagene) and standard amplification conditions. Forward primers contained a SnaBI restriction site: 5'-ggggtacgtagccaccatgcgaccctccgggacggccggg-3' for EGFR and 5'-ggggtacgtagccaccatggagctggcggccttgtgccgc-3' for ErbB2. The reverse primers contained an EcoRI restriction site: 5'-cgcggaattcctacagatcctcttctgagatgag-3' for both EGFR and ErbB2. The reverse primer was designed to also incorporate an in-frame myc tag at the 3' end of EGFR and ErbB2. EGFR was cloned into the *SnaBI* and *EcoRI* sites of pBabe Puro and ErbB2 was cloned into the *SnaBI* and *EcoRI* sites of pBabe Hygro vector. Both pBabe vectors were generously donated by Dr. Margaret Frame (The Beatson Institute for Cancer research, Glasgow, UK).

Library Construction.

The EGFR fragment (residues 613-1036) was randomly mutated using the EzClone Domain Mutagenesis kit (Stratagene) as recommended by the manufacturer. Forward 5'-agacgccggccatgtgtgccacc-3' and reverse 5'-cagagagctcaggaggggagtcc-3' primers were used for the error-prone PCR. The EzClone reaction (50 μl) was performed using 50 ng of EGFR-pBabe Puro plasmid and 500 ng of mutated PCR product. Non-mutated plasmid was digested with DpnI (New England Biolabs). The library was transformed into Maximum Efficiency DH5α cells (Invitrogen) and plasmid DNA extracted using Qiagen extraction kits.

Resistance Mutation Screens.

1 x10^6 Ba/F3 or Ba/F3/ErbB2 cells were infected with the EGFR mutation library to achieve 30- 40% infection efficiency in order to avoid multiple proviral integrations in each cell. Infected cells were washed twice with PBS before being resuspended in RPMI 1640 medium supplemented with 10% (v/v) fetal calf serum, 20 ng/ml EGF, 0.24% (w/v) agar (USB Corporation) and the respective EGFR inhibitor. Erlotinib was used at final concentrations of 2 μM and 3.2 μM, lapatinib at 4 μM and CI-1033 at 0.1 μM and 0.15 μM. For EGFR mutation screening in the ErbB2 background, erlotinib was applied at 2.5 μM, lapatinib at 4.5 μM and CI-1033 at 0.1 μM. Cells were incubated at 37ºC for 10- 15 days to allow resistant colonies to develop. After isolation and expansion of drug resistant colonies, genomic DNA was extracted using a Generation capture column kit (Gentra). The EGFR cytoplasmic

domain was PCR amplified using forward 5' caacaccctggtctggaagt and reverse 5' gggtcctacagatcctcttctg primers and sequenced in both directions. Mutations were mapped onto the publicly available EGFR crystal structures to highlight potential mutations of particular interest and these were re-introduced into EGFR-myc-pBabe using the QuickChange mutagenesis kit (Strategene) to allow further functional characterisation.

Cell Viability Assay.

Mixed populations of Ba/F3 cells expressing either wild type EGFR or EGFR containing the desired point mutations were plated at 1 x10^5 cells per well in triplicate and incubated with increasing concentrations of erlotinib (0, 0.001, 0.003, 0.01, 0.03, 0.1, 0.3, 1, 3 and 10 μM), lapatinib (0, 0.001, 0.003, 0.01, 0.03, 0.1, 0.3, 1, 3 and 5μM) and CI-1033 (0, 0.001, 0.003, 0.01, 0.03, 0.1, 0.3, 1, 3 and 10 μM). Due to the increased sensitivity of EGFR-L858R to EGFR inhibitors, cells expressing EGFR-L858R were exposed to lower concentrations of erlotinib (0, 0.0003, 0.001, 0.003, 0.01, 0.03, 0.1, 0.3, 1 and 3 μM) and CI-1033 (0, 0.03, 0.1, 0.3, 1, 3, 10, 30, 100 and 300 nM). The extent of cell proliferation was measured using a methanethiosulfonate (MTS)-based cell viability assay (CellTiter96 Aqueous One Solution Reagent; Promega). The raw absorbance values were used to determine the concentration of drug required to inhibit 50% of cell viability using the software package Origin (OriginLab). All IC_{50} values presented in the paper are means of at least two independent experiments.

Immunoblotting and Immunoprecipitation.

6 x10^6 cells were lysed in buffer containing 25 mM Tris (pH 7.4), 150 mM NaCl, 0.27 M sucrose, 1% (v/v) Triton X-100, 0.1% (w/v) SDS, 3 mM EDTA, 3 mM EGTA, 10 mM β-glycerophosphate, 5 mM pyrophosphoate, 0.1% (v/v) β-mercaptoethanol, protease inhibitor cocktail (Roche), 2 mM sodium orthovanadate and 5 mM sodium fluoride and clarified by centrifugation at 4°C. Proteins were separated by 4-20% SDS-PAGE (Bio-Rad), transferred to Hybond-C Extra membrane (Amersham), blocked with TBST containing 5% (v/v) FCS, and probed with the relevant antibody. The antibodies used were 1:1000 rabbit polyclonal anti-phospho-Y1068-EGFR (Biosource) and 1:1000 mouse monoclonal anti-myc (clone 9E10) or 1:1000 rabbit polyclonal anti-phospho-Y1248-ErbB2 (Cell Signalling Technology) and 1:1000 anti-myc antibodies. The anti-phospho-Y1068-EGFR antibody recognises EGFR phosphorylated on Y1068 of the mature human isoform 1 which corresponds to Y1092 from the precursor form.

ErbB2 was immunoprecipitated from lysates prepared from 6 x10^6 Ba/F3/ErbB2 or Ba/F3/EGFR+ErbB2 cells and incubated with 1.5 μg of anti-myc antibody overnight at 4ºC, followed by incubation with Protein-G sepharose (Sigma-Aldrich) for 1 hour. The immune complexes were probed with 1:1000 rabbit polyclonal phospho–Y1248-ErbB2 and 1:1000 anti-myc antibodies.

All immunoblots were probed with respective secondary antibodies. Goat anti-rabbit IRDye800 (Li-Cor Biosciences) was used at 1:10000 and goat anti-mouse IRDye680 (Li-Cor Biosciences) was used at 1:5000. Individual blots were scanned in the linear detection range using the Odyssey infrared imaging system (Li-COR Biosciences) with both the 700 and 800 nm channels being captured in a single scan for each image. The signal changes in each image are therefore linear.

Computational Tools.

All protein structure diagrams were created using the Maestro package from Schrodinger. (Schrodinger, San Diego).

Results

Activation of EGFR and ErbB2 leads to IL-3-independent Ba/F3 cell growth.

Previous reports demonstrated that expression of wild-type (wt) EGFR or activated EGFR-L858R in Ba/F3 cells is sufficient for IL-3-independent growth [6]. We therefore generated Ba/F3 cell lines stably expressing either wt EGFR, EGFR-L858R or ErbB2. To address whether ErbB2 can modulate EGFR's sensitivity to inhibitors we also generated Ba/F3 lines co-expressing EGFR and ErbB2. Expression was verified by Western blotting (Figure 2a), with only EGFR-L858R displaying detectable Y1092 phosphorylation in the absence of EGF (Figures 2a and b) confirming that this mutant is not dependent upon ligand. EGFR, EGFR and ErbB2, and EGFR-L858R cells all exhibited comparable levels of phospho-Y1092 EGFR when exposed to EGF (Figure 2b). Significant phospho-Y1248 ErbB2 levels were observed in EGF stimulated cells co-expressing EGFR and ErbB2 (Figure 2c), whilst phosphorylated ErbB2 was also detected in Ba/F3/ErbB2 cells exposed to heregulin (Figure 2d). ErbB3 mRNA has previously been detected in Ba/F3 cells [16] suggesting that low levels of ErbB3 protein are present and capable of activating ErbB2 in a heregulin-dependent manner.

Ba/F3 cells expressing EGFR, EGFR and ErbB2, and ErbB2 proliferated at a similar rate in a ligand dependent manner, whilst EGFR-L858R cells grew slightly faster irrespective of the presence of EGF (Figure 2e). These results confirm previous reports that ErbB family members and mutants render Ba/F3 cells IL-3-independent and act as oncogenic stimuli [17].

Next we examined inhibition of EGFR signalling by erlotinib, lapatinib and CI-1033. Ba/F3 cells expressing ErbB family members were exposed to each inhibitor for 48h before cell viability was assessed in order to determine the IC_{50} of each inhibitor. For all EGFR expressing cell lines the inhibitor potencies ranked in the following order: CI-1033 >>erlotinib >lapatinib (Table 1). Introduction of L858R into EGFR led to a 10- 15-fold increase in sensitivity to erlotinib and CI-1033, whilst lapatinib was unaffected (Table 1). Co-expression of EGFR with ErbB2 in the presence of EGF didn't influence erlotinib or CI-1033 potency, but increased sensitivity to lapatinib 4-fold (Table 1). ErbB2 cells stimulated with heregulin were sensitive to both lapatinib and CI-1033 (Table1). Since each inhibitor was characterised using mixed populations of cells generated on several occasions, a degree of variation in the expression levels of each EGFR mutant was expected. Inhibitor IC_{50}'s were therefore measured on multiple occasions and the IC_{50} values obtained were reproducible with at most a two-fold variation being observed between individual experiments. This suggests that the expression levels of EGFR had little impact upon the IC_{50} value obtained and supports the conclusion that the varying abilities of erlotinib, lapatinib and CI-1033 to inhibit EGFR driven proliferation are due to their differing affinities for the various forms of EGFR.

EGFR resistance mutation screens with erlotinib, lapatinib and CI-1033.

We used error-prone PCR to generate a library consisting of EGFR randomly mutated within its transmembrane, juxtamembrane and kinase domains. We focussed upon these domains in order to specifically examine the direct structure/ function relationship of the kinase domain with the various EGFR inhibitors. It is likely that by

adopting this strategy we may have missed residues in the extra-cellular domain that could potentially cause drug resistance through indirect effects upon the conformation of the kinase domain.

We estimate the library contained approximately 66,000 clones with approximately one base pair change in each target sequence. Ba/F3 cells were infected with the EGFR mutation library and drug resistant colonies selected following previously published techniques [15]. The concentrations of erlotinib (2 and 3.2 μM), lapatinib (4 μM) and CI-1033 (0.1 and 0.15 μM) used in the screens were chosen to reflect the reported maximal drug plasma concentrations observed in the clinic [12,18,19]. Maximal concentrations of lapatinib were limited to 5 μM throughout this study, since higher concentrations resulted in cell death of Ba/F3 cells (data not shown). To determine the impact of ErbB2 upon EGFR resistance we also infected Ba/F3 cells stably expressing ErbB2 with the EGFR mutation library and selected for drug resistant growth in the presence of erlotinib (2.5 μM), lapatinib (4.5 μM) and CI-1033 (0.1 μM).

Following each screen, resistant clones were picked, expanded and analysed by direct sequencing. Each inhibitor yielded differing proportions of mutated versus wild-type EGFR containing colonies in the various screens performed. 95-100% of the resistant clones generated by erlotinib contained mutations, lapatinib yielded 75-82% and exposure to CI-1033 resulted in 79-91% of the colonies containing mutations. Since we only sequenced the cytoplasmic domain of EGFR it is conceivable that those colonies that were apparently wild-type could possibly contain mutations in the extracellular portion of EGFR. Alternatively, other mechanisms of drug resistance such as the up regulation of drug transporter proteins, increase in EGFR expression level or activation of other signalling pathways may have contributed to drug resistance in the "wild-type" colonies.

In total we discovered 40 mutated residues (Figure 3a). Since crystal structures of EGFR complexed with either erlotinib, lapatinib or 13-JAB (an irreversible inhibitor related to CI-1033) are available [9,10], we mapped mutations that were localized within drug contact regions or specific functional regions of the kinase domain onto these crystal structures (Figures 3b-d). Erlotinib, lapatinib and CI-1033 all interact with the EGFR hinge region through the quinazoline ring, whilst the anilino group is orientated towards the selectivity pocket. The anilino group of lapatinib is extended when compared to erlotinib and CI-1033 resulting in it binding much deeper into the selectivity pocket. CI-1033 differs significantly from both erlotinib and lapatinib at the quinazoline 6-position where it contains a reactive group that forms a direct covalent bond with C797 [20].

Mutation of the gatekeeper residue (T790M) was detected with varying frequencies in all six screens, although it was most prevalent with erlotinib (Figure 3a, Supplementary Figure 1a). Mutations of M766, T854, L718, and G796 were also identified in the erlotinib resistance screen (Figure 3a) and each of these residues makes direct contact with erlotinib (Figure 3b). Interestingly, we also identified a number of erlotinib resistant mutations (L777M, E762V/G, V769L, K852T/E and A859D) only in the presence of ErbB2 (Figure 3a). In contrast, CI-1033 and lapatinib appeared less sensitive to the presence of ErbB2 presumably because they are both very efficient ErbB2 inhibitors.

Lapatinib yielded the broadest mutation spectra of any of the inhibitors tested in our *in vitro* system (Figure 3a, Supplementary Figure 1b). Some of the mutated residues (e.g. T790, L718, V769, L777, and T854) overlapped with the erlotinib and/or CI-1033 screens (Figure 3a) emphasizing the chemical similarities of the drug

cores. However, there were a number of mutations (E709G, L747S, D770Y, H773L, C775F, R776P, L788I/V, K860T, G863S and R889S) that were unique to lapatinib (Figure 3a). The majority of these unique mutations clustered in and around the selectivity pocket (L747, C775, R776, L777 and L788) or on the EGFR activation loop (K860, G863 and R889) (Figure 3c) suggesting that these regions may be particularly important for lapatinib binding. Comparison of the ratio of contact residues versus non-contact residues for each inhibitor also suggested that binding of lapatinib significantly differed from both erlotinib and CI-1033. The majority (75%) of residues mutated as a consequence of exposure to lapatinib didn't directly contact ligand whilst this frequency was dramatically lower with erlotinib (25%) and CI-1033 (50%).

Mapping of the CI-1033 resistance mutants onto the EGFR-13-JAB structure highlighted three interesting resistance clusters. The first cluster (C797S/G, G796R/C and P794L) was located near CI-1033's solubilising and reactive groups (Figure 2d). C797 was the most frequently mutated residue identified in our CI-1033 screens (Supplementary Figure 1c). C797 is critical for irreversible inhibitor binding [21], since it contains the –SH group that reacts with CI-1033 to form the covalent bond. G796 is positioned adjacent to the critical C797 whilst P794 is located close to the morpholine group of CI-1033. The second mutation cluster (T790M and M766V/T) is located close to the aniline group of CI-1033 (Figure 3d). Interestingly, T790M mutation was significantly less prevalent in the CI-1033 screen when compared to the erlotinib screen (Supplementary Figure 1c). The final cluster observed (V742A, A743S and I744F) was located above CI-1033's quinazoline ring (Figure 3d).

The impact of EGFR mutations upon drug sensitivity.

Having mapped the resistance mutations obtained in our screens we sought to determine the degree of resistance conferred by selected mutations to erlotinib, lapatinib and CI-1033. Mutations T790M (gatekeeper), M766T (C-helix), L718A (solvent chanel) and T854A (activation loop) were most prevalent in the erlotinib screen, while mutations G796R and C797S (solvent chanel) were most frequently detected in the CI-1033 screen (Supplementary Figures 1a and c). We introduced these EGFR variants into Ba/F3 cells for further testing of drug resistance. We also chose H773L, -R776P, -L777Q and -L788V mutations, since they were identified only in the lapatinib screen. In addition, we took advantage of the fact that co-expression of ErbB2 markedly lowered the IC_{50} of lapatinib in order to overcome the limitations imposed by its cellular toxicity.

All cell lines were treated with increasing doses of erlotinib, lapatinib and CI-1033 to generate cell proliferation dose response curves. As expected, EGFR-T790M was highly resistant to erlotinib and lapatinib (Table 2 and Supplementary Figures 2a and b). In contrast, CI-1033 remained an effective inhibitor of Ba/F3/EGFR-T790M cell proliferation despite its IC_{50} being increased 10.8-fold (Table 2 and Supplementary Figure 2c). The effect of M766T, L718A and T854A upon erlotinib and CI-1033 potency was much more moderate with only a 3-8-fold IC_{50} increase being observed (Table 2 and Supplementary Figures 2a and c). L718A and T854A conferred resistance to lapatinib, whilst M766T slightly sensitized EGFR to lapatinib (Table 2 and Supplementary Figure 2b). G796R increased resistance to CI-1033 100-fold supporting the significance of this residue in the covalent bond formed by the adjacent C797 (Table 2 and Supplementary Figure 2c). Mutation of G796 was also detected in the erlotinib screen and decreased the potency of both lapatinib and erlotinib (Table 2 and Supplementary Figures 2a and b) indicating that this residue

adversely affects groups on the 6/ 7 positions of the quinazoline ring. As expected, the C797S mutation severely affected CI-1033 binding resulting in a ~170-fold increase in the growth IC_{50} (Table 2 and Supplementary Figure 3c).

Co-expression of ErbB2 with EGFR-H773L, -R776P, -L777Q and -L788V displayed complete resistance to lapatinib (Table 4 and Supplementary Figure 4b) thus substantiating the importance of the selectivity pocket for lapatinib binding. Furthermore lapatinib treatment of Ba/F3 cells co-expressing EGFR-L788V and ErbB2 failed to completely inhibit EGFR Y1092 phosphorylation at concentrations 6-fold higher than the wild-type IC_{50} (Figure 4) thus confirming lapatinibs inability to directly inhibit these selectivity pocket mutants.

The relationship between L858R and drug resistant mutants.

To assess the potential clinical impact of T790M, -M766T, -L718A, -T854A, -G796R and -C797S upon drug sensitivity these mutations were introduced into the clinically relevant EGFR-L858R background. In addition, we also generated EGFR-T790M-C797S-L858R to investigate how combination of the two most prevalent erlotinib and CI-1033 resistance mutations affected drug sensitivity. The overall pattern of resistance conferred by T790M was similar in both the wild type EGFR and L858R background (Tables 2 and 3). Inhibition of EGFR-L858R or EGFR-L858R-T790M Y1092 phosphorylation in cells following erlotinib or CI-1033 treatment correlated well with the IC_{50} values determined in our proliferation assays (Figure 4 and Table 3) confirming that drug resistance was primarily driven by EGFR mutation. A similarly decreased sensitivity to irreversible inhibitors was also recently reported with EGFR-L858R-T790M treated with HKI-272 [21].

Combination of either M766T or G796R with L858R severely affected cell proliferation (data not shown) indicating that both mutations when combined with L858R impair EGFR activity. Although resistance to erlotinib and CI-1033 was observed with EGFR-L858R-M766T, this mutant surprisingly sensitized EGFR to lapatinib (Table 3 and Supplementary Figure 3). L858R-L718A conferred significant resistance to erlotinib (17.3-fold increase) and CI-1033 (11.2-fold increase), while L858R-T854A demonstrated less resistance to all tested inhibitors when compared to L858R-L718A (Table 3 and Supplementary Figures 3a-c). Similar to wt EGFR, the introduction of C797S into L858R dramatically impaired EGFR inhibition by CI-1033 as assessed by both proliferation and Y1092 phosphorylation (Table 3 and Figure 4). Complete resistance to all inhibitors at the maximum tolerated doses was achieved when T790M and C797S mutations were combined in the L858R mutation background (Table 3) demonstrating how results from these screens can be used to predict structure/ function relationships.

The Impact of ErbB2 Upon EGFR Drug Resistance.

Since E762V, V769L and K852T mutations were detected in the erlotinib screen performed in the presence of ErbB2, we examined the relationship between these mutations and ErbB2. To evaluate their effect we expressed and characterised EGFR-E762V, -V769L and -K852T in the presence or absence of ErbB2. Ba/F3 cells infected with EGFR-E762V did not survive in IL-3-free medium supplemented with EGF suggesting that activation of EGFR was severely impaired by mutation of this important residue. Unexpectedly, co-expression of ErbB2 with EGFR-E762V resulted in viable cells that were mildly resistant to erlotinib and significantly more sensitive to lapatinib (Table 4 and Supplementary Figures 4a and b). Co-expression of ErbB2 with EGFR-V769L consistently increased the level of resistance observed with

erlotinib, lapatinib and CI-1033 (Tables 2 and 4, and Figure 4b). EGFR-K852T conferred mild resistance to erlotinib (Table 2), but much more significant increases in erlotinib, lapatinib and CI-1033 resistance (5-8-fold) were observed when K852T was co-expressed with ErbB2 (Table 4 and Supplementary Figures 4a-c). This increased resistance was consistent with K852T only being identified in screens where ErbB2 was present.

Combination of erlotinib and CI-1033 significantly reduces drug resistant colony formation.

We established that the key erlotinib resistance mutation is T790M whilst mutations of C797S and G796R strongly impaired inhibition by CI-1033. We predicted that combination of erlotinib and CI-1033 should significantly reduce the number of resistant clones since proliferation of cells expressing EGFR-T790M was potently inhibited by CI-1033 whilst erlotinib efficiently inhibited C797S. The resistance screen was therefore repeated in the presence of various concentrations of erlotinib and CI-1033. We observed that increasing concentrations of either erlotinib or CI-1033 inversely correlated with the number of resistant colonies obtained (Figure 5). As predicted, the combination of erlotinib with CI-1033 was extremely effective in preventing the formation of resistant colonies presumably because each inhibitor exerts selective pressure in a complementary manner (Figure 5).

Discussion

Our study of EGFR drug resistant mutations demonstrates that erlotinib, lapatinib and CI-1033 each yield a different mutational profile despite the overall similarity in their chemical structures. For erlotinib, the primary resistance hotspot is observed at the entrance to the selectivity pocket whilst lapatinib resistant mutations were clustered deep in the selectivity pocket and on the activation loop. CI-1033 was exquisitely sensitive to mutations on and around C797, where the covalent bond is formed. T790M was the only mutation consistently identified in all of our screens thus confirming the importance of the gatekeeper residue in drug resistance. The exact mechanism through which T790M blocks drug binding is not completely understood, though steric interference caused by the bulkier methionine residue is thought to contribute [22]. The importance of the selectivity pocket in determining erlotinib binding is emphasized by the prevalence of M766 and T854 mutations in our resistance screens. M766 forms part of the pocket in which the anilino group of erlotinib binds and substitution by the hydrophilic threonine would likely affect the electrostatic nature of the pocket, whilst substitution with valine may affect the shape of the pocket. Furthermore, M766T/V is particularly interesting since it resides on the C-helix of EGFR suggesting that it may additionally influence the equilibrium between C-helix 'in' and 'out' conformations thus differentially affecting the binding affinity for either ATP or erlotinib. Mutation of T854 to the smaller, hydrophilic alanine may increase the size of the selectivity pocket thus negatively impacting erlotinib binding.

Although our studies with lapatinib were limited by its cellular toxicity it consistently yielded a broader spectrum of mutations than CI-1033 or erlotinib. Many of the most prevalent lapatinib resistant mutations clustered in and around the EGFR selectivity pocket highlighting the importance of this region for binding of kinase inhibitors with extended aniline groups. This finding is exemplified by L747 and R776, which localize deep in the selectivity pocket. Similar to erlotinib and CI-1033, residues such as C775, L777 and L788 that directly contact ligand are prone to

mutation as an escape mechanism. For example, C775 substitution with the bulkier phenylalanine may cause a steric clash with the aniline group and L777Q mutation involves replacement of a hydrophobic residue with a hydrophilic one, thereby reducing lapatinib's potency since the binding of the anilino group appears principally driven through hydrophobic interactions.

Upon close examination of the overall proportion of contact versus non-contact residues combined with the location of each mutation we noticed that mutations that affect the conformation of EGFR might offer an additional resistance mechanism to lapatinib. This mechanism appears unique to lapatinib (when compared with erlotinib and CI-1033) and is suggested by the low frequency (25%) of mutated contact residues (Fig.3A) and their structural location. For instance, mutations preceding the EGFR C-helix (e.g. D770Y, R776P and H773L) may influence the conformation state of EGFR and thus prevent lapatinib binding. For example, H773L mutation may favour the C-helix "in" confirmation consequently disfavouring lapatinib binding whilst activation loop mutations (e.g. T854S, K860T, G863S and R889S) may also influence the C-helix "in"/ "out" conformational equilibrium as studies with Abl indicate that the movements of the activation loop and C-helix might be correlated [23].

Our discovery that lapatinib consistently generated a broad mutation spectrum is analogous to that demonstrated with imatinib [24]. This similarity supports the finding that inhibitors that make extensive use of the selectivity pocket (e.g. lapatinib) and preferentially bind to an inactive conformation are more vulnerable to resistance mutations. This highlights an apparent conflict in the design of kinase inhibitors, since approaches to gain maximum kinase selectivity usually involve interacting with residues distal from the ATP binding site within the selectivity pocket. This situation is perhaps best illustrated by comparing imatinib with the Aurora kinase inhibitor VX-680 [25]. VX-680 does not significantly interact with the selectivity pocket and is therefore able to overcome a number of BCR-Abl mutations including T315I [25]. However, since it interacts with residues that are in contact with ATP its kinase selectivity profile is much broader than imatinib's [5].

Resistance to CI-1033 was dominated by mutation of residues located near CI-1033's solubilising and reactive groups. CI-1033 was exquisitely sensitive to C797S mutation since C797 is critical for irreversible inhibitor binding. Although serine contains an –OH side chain that is potentially available for covalent reaction, serine is much less chemically reactive when compared to cysteine. Mutations or residues around C797 (e.g. G796R/C and P794L) may also interfere with the ability of CI-1033 to form covalent interaction by affecting the conformation and/or accessibility of the key C797 residue.

In our study we frequently observed C797S and G796R/C mutations and confirmed that they are the key mutations involved in CI-1033 resistance. In contrast to our findings, a study by Yu *et al.* did not identify C797 mutation in L858R-T790M-mutant lung adenocarcinoma cells adapted for resistance to the irreversible inhibitor CL-387,785 [26]. In addition, cells engineered by Yu *et al*. to express EGFR-T790M-L858R-C797S conferred only mild resistance to CL-387,785 [26]. There are several explanations for these differences. One possibility is simply that CI-1033 and CL-387,785 are structurally distinct and may therefore behave differently in a cellular environment. Alternatively, since our data suggests that the presence of EGFR binding partners (e.g. ErbB2) can modulate the resistance spectrum by either promoting the survival of a drug resistant mutant (e.g. EGFR-E762V) or rendering a particular mutant markedly more drug resistant (e.g. EGFR-K852T) it is conceivable

that the interacting proteins present in the cell lines used in the screens differed sufficiently to influence both the resistance mutation profile and the degree of resistance obtained.

Several of the hypotheses we have proposed for the mechanisms by which the various mutations confer drug resistance are speculative predictions based upon structural models or previous findings with BCR-Abl. It is possible that other explanations exist to rationalize our findings. For example, increased expression of BCR-Abl results in imatinib resistance [27]. Perhaps some of our resistance mutations could stabilize EGFR, resulting in increased protein levels and resistance to the various inhibitors tested. Definitive proof of the precise mechanisms underlying drug resistance will require a variety of cellular, biochemical and crystallographic techniques to study each mutation in further detail and we await the outcomes of these studies with interest.

Numerous ErbB family irreversible inhibitors are currently being investigated as a method to overcome clinical resistance driven by T790M mutation of EGFR [28]. Our screening data with the irreversible inhibitor CI-1033 indicates that clinical resistance to this class of inhibitor is possible and we expect that incidences of EGFR-G796 and -C797 mutations will be reported in the clinic following prolonged exposure to irreversible inhibitors. Interestingly, alignment of the ErbB2 and EGFR kinase domains indicates that many of the lapatinib and CI-1033 resistance residues are conserved in ErbB2 (Supplementary Figure 4). This suggests that clinical resistance (either acquired or intrinsic) due to ErbB2 mutations is a likely possibility in ErbB2 driven tumours treated with either lapatinib or irreversible inhibitors. Based upon our study we predict that ErbB2-C805 will be observed in response to irreversible inhibitors whilst lapatinib will yield a broad range of mutations that will likely include the gatekeeper (ErbB2-T798) and residues clustered deep in the selectivity pocket.

Combinations of drugs that bind to different conformations of BCR-Abl have been demonstrated preclinically to be an effective method of reducing the frequency of resistance mutations [24,29]. Our *in vitro* data suggests that if the toxicity could be tolerated then a combination of erlotinib/ gefitinib and an irreversible inhibitor in first-line therapy might be a useful approach to prevent expansion of resistant clones harbouring T790M or C797S mutations. However, if T790M and C797S were mutated in the same EGFR allele then complete resistance to current EGFR kinase inhibitors would probably occur. If EGFR driven NSCLC behaves similarly to BCR-Abl driven CML then the chances of acquiring multiple resistance mutations in the same EGFR allele would probably be heightened if the EGFR targeted therapies were applied in a sequential manner. This scenario has very recently been observed in CML patients treated with imatinib, dasatinib and nilotinib [30-32]. It is probable that the outcome of future combination trials in resistant disease will determine whether the combination of targeted therapies that inhibit distinct molecular targets will unlock their full potential to deliver significant patient benefit.

Acknowledgements

This study was fully funded by AstraZeneca and all authors were employees of AstraZeneca at the time of writing.

Abbreviations

CML, chronic myeloid leukaemia; EGF, epidermal growth factor; EGFR, EGF receptor; IL-3, interleukin 3; NSCLC, non-small cell lung cancer.

Reference List

1 Baselga, J. (2006) Targeting tyrosine kinases in cancer: the second wave. Science **312**, 1175-1178

2 O'Hare, T., Corbin, A. S. and Druker, B. J. (2006) Targeted CML therapy: controlling drug resistance, seeking cure. Curr Opin.Genet.Dev **16**, 92-99

3 Sharma, S. V., Bell, D. W., Settleman, J. and Haber, D. A. (2007) Epidermal growth factor receptor mutations in lung cancer. Nat.Rev.Cancer **7**, 169-181

4 Kwak, E. L., Sordella, R., Bell, D. W., Godin-Heymann, N., Okimoto, R. A., Brannigan, B. W., Harris, P. L., Driscoll, D. R., Fidias, P., Lynch, T. J., Rabindran, S. K., McGinnis, J. P., Wissner, A., Sharma, S. V., Isselbacher, K. J., Settleman, J. and Haber, D. A. (2005) Irreversible inhibitors of the EGF receptor may circumvent acquired resistance to gefitinib. Proc.Natl.Acad.Sci.U S A **102**, 7665-7670

5 Carter, T. A., Wodicka, L. M., Shah, N. P., Velasco, A. M., Fabian, M. A., Treiber, D. K., Milanov, Z. V., Atteridge, C. E., Biggs, W. H., III, Edeen, P. T., Floyd, M., Ford, J. M., Grotzfeld, R. M., Herrgard, S., Insko, D. E., Mehta, S. A., Patel, H. K., Pao, W., Sawyers, C. L., Varmus, H., Zarrinkar, P. P. and Lockhart, D. J. (2005) Inhibition of drug-resistant mutants of ABL, KIT, and EGF receptor kinases. Proc.Natl.Acad.Sci.U S A **102**, 11011-11016

6 Kobayashi, S., Ji, H., Yuza, Y., Meyerson, M., Wong, K. K., Tenen, D. G. and Halmos, B. (2005) An alternative inhibitor overcomes resistance caused by a mutation of the epidermal growth factor receptor. Cancer Res. **65**, 7096-7101

7 Erlichman, C., Hidalgo, M., Boni, J. P., Martins, P., Quinn, S. E., Zacharchuk, C., Amorusi, P., Adjei, A. A. and Rowinsky, E. K. (2006) Phase I study of EKB-569, an irreversible inhibitor of the epidermal growth factor receptor, in patients with advanced solid tumors. J.Clin.Oncol. **24**, 2252-2260

8 Reid, A., Vidal, L., Shaw, H. and de Bono, J. (2007) Dual inhibition of ErbB1 (EGFR/HER1) and ErbB2 (HER2/neu). Eur.J.Cancer **43**, 481-489

9 Stamos, J., Sliwkowski, M. X. and Eigenbrot, C. (2002) Structure of the epidermal growth factor receptor kinase domain alone and in complex with a 4-anilinoquinazoline inhibitor. J.Biol.Chem. **277**, 46265-46272

10 Wood, E. R., Truesdale, A. T., McDonald, O. B., Yuan, D., Hassell, A., Dickerson, S. H., Ellis, B., Pennisi, C., Horne, E., Lackey, K., Alligood, K. J., Rusnak, D. W., Gilmer, T. M. and Shewchuk, L. (2004) A unique structure for epidermal growth factor receptor bound to GW572016 (Lapatinib): relationships among protein conformation, inhibitor off-rate, and receptor activity in tumor cells. Cancer Res. **64**, 6652-6659

11 Smaill, J. B., Showalter, H. D., Zhou, H., Bridges, A. J., McNamara, D. J., Fry, D. W., Nelson, J. M., Sherwood, V., Vincent, P. W., Roberts, B. J., Elliott, W.

L. and Denny, W. A. (2001) Tyrosine kinase inhibitors. 18. 6-Substituted 4-anilinoquinazolines and 4-anilinopyrido[3,4-d]pyrimidines as soluble, irreversible inhibitors of the epidermal growth factor receptor. J.Med.Chem. **44**, 429-440

12 Burris, H. A., III, Hurwitz, H. I., Dees, E. C., Dowlati, A., Blackwell, K. L., O'Neil, B., Marcom, P. K., Ellis, M. J., Overmoyer, B., Jones, S. F., Harris, J. L., Smith, D. A., Koch, K. M., Stead, A., Mangum, S. and Spector, N. L. (2005) Phase I safety, pharmacokinetics, and clinical activity study of lapatinib (GW572016), a reversible dual inhibitor of epidermal growth factor receptor tyrosine kinases, in heavily pretreated patients with metastatic carcinomas. J.Clin.Oncol. **23**, 5305-5313

13 Hirsch, F. R., Varella-Garcia, M., Bunn, P. A., Jr., Franklin, W. A., Dziadziuszko, R., Thatcher, N., Chang, A., Parikh, P., Pereira, J. R., Ciuleanu, T., von Pawel, J., Watkins, C., Flannery, A., Ellison, G., Donald, E., Knight, L., Parums, D., Botwood, N. and Holloway, B. (2006) Molecular predictors of outcome with gefitinib in a phase III placebo-controlled study in advanced non-small-cell lung cancer. J.Clin.Oncol. **24**, 5034-5042

14 Zinner, R. G., Nemunaitis, J., Eiseman, I., Shin, H. J., Olson, S. C., Christensen, J., Huang, X., Lenehan, P. F., Donato, N. J. and Shin, D. M. (2007) Phase I clinical and pharmacodynamic evaluation of oral CI-1033 in patients with refractory cancer. Clin.Cancer Res. **13**, 3006-3014

15 Azam, M., Latek, R. R. and Daley, G. Q. (2003) Mechanisms of autoinhibition and STI-571/imatinib resistance revealed by mutagenesis of BCR-ABL.[see comment]. Cell **112**, 831-843

16 Riese, D. J., van Raaij, T. M., Plowman, G. D., Andrews, G. C. and Stern, D. F. (1995) The cellular response to neuregulins is governed by complex interactions of the erbB receptor family. Mol.Cell Biol. **15**, 5770-5776

17 Greulich, H., Chen, T. H., Feng, W., Janne, P. A., Alvarez, J. V., Zappaterra, M., Bulmer, S. E., Frank, D. A., Hahn, W. C., Sellers, W. R. and Meyerson, M. (2005) Oncogenic transformation by inhibitor-sensitive and -resistant EGFR mutants. PLoS Med. **2**, e313

18 Calvo, E., Tolcher, A. W., Hammond, L. A., Patnaik, A., de Bono, J. S., Eiseman, I. A., Olson, S. C., Lenehan, P. F., McCreery, H., Lorusso, P. and Rowinsky, E. K. (2004) Administration of CI-1033, an irreversible pan-erbB tyrosine kinase inhibitor, is feasible on a 7-day on, 7-day off schedule: a phase I pharmacokinetic and food effect study. Clin.Cancer Res. **10**, 7112-7120

19 Hamilton, M., Wolf, J. L., Rusk, J., Beard, S. E., Clark, G. M., Witt, K. and Cagnoni, P. J. (2006) Effects of smoking on the pharmacokinetics of erlotinib. Clin.Cancer Res. **12**, 2166-2171

20 Smaill, J. B., Rewcastle, G. W., Loo, J. A., Greis, K. D., Chan, O. H., Reyner, E. L., Lipka, E., Showalter, H. D., Vincent, P. W., Elliott, W. L. and Denny, W. A. (2000) Tyrosine kinase inhibitors. 17. Irreversible inhibitors of the epidermal

growth factor receptor: 4-(phenylamino)quinazoline- and 4-(phenylamino)pyrido[3,2-d]pyrimidine-6-acrylamides bearing additional solubilizing functions. J.Med.Chem. **43**, 1380-1397

21 Ji, H., Zhao, X., Yuza, Y., Shimamura, T., Li, D., Protopopov, A., Jung, B. L., McNamara, K., Xia, H., Glatt, K. A., Thomas, R. K., Sasaki, H., Horner, J. W., Eck, M., Mitchell, A., Sun, Y., Al Hashem, R., Bronson, R. T., Rabindran, S. K., Discafani, C. M., Maher, E., Shapiro, G. I., Meyerson, M. and Wong, K. K. (2006) Epidermal growth factor receptor variant III mutations in lung tumorigenesis and sensitivity to tyrosine kinase inhibitors. Proc.Natl.Acad.Sci.U S A **103**, 7817-7822

22 Kobayashi, S., Boggon, T. J., Dayaram, T., Janne, P. A., Kocher, O., Meyerson, M., Johnson, B. E., Eck, M. J., Tenen, D. G. and Halmos, B. (2005) EGFR mutation and resistance of non-small-cell lung cancer to gefitinib. N.Engl.J.Med. **352**, 786-792

23 Levinson, N. M., Kuchment, O., Shen, K., Young, M. A., Koldobskiy, M., Karplus, M., Cole, P. A. and Kuriyan, J. (2006) A Src-like inactive conformation in the abl tyrosine kinase domain. PLoS Biol. **4**, e144

24 Burgess, M. R., Skaggs, B. J., Shah, N. P., Lee, F. Y. and Sawyers, C. L. (2005) Comparative analysis of two clinically active BCR-ABL kinase inhibitors reveals the role of conformation-specific binding in resistance. Proc.Natl.Acad.Sci.U S A **102**, 3395-3400

25 Young, M. A., Shah, N. P., Chao, L. H., Seeliger, M., Milanov, Z. V., Biggs, W. H., III, Treiber, D. K., Patel, H. K., Zarrinkar, P. P., Lockhart, D. J., Sawyers, C. L. and Kuriyan, J. (2006) Structure of the kinase domain of an imatinib-resistant Abl mutant in complex with the Aurora kinase inhibitor VX-680. Cancer Res. **66**, 1007-1014

26 Yu, Z., Boggon, T. J., Kobayashi, S., Jin, C., Ma, P. C., Dowlati, A., Kern, J. A., Tenen, D. G. and Halmos, B. (2007) Resistance to an irreversible epidermal growth factor receptor (EGFR) inhibitor in EGFR-mutant lung cancer reveals novel treatment strategies. Cancer Res. **67**, 10417-10427

27 Le Coutre, P., Tassi, E., Varella-Garcia, M., Barni, R., Mologni, L., Cabrita, G., Marchesi, E., Supino, R. and Gambacorti-Passerini, C. (2000) Induction of resistance to the Abelson inhibitor STI571 in human leukemic cells through gene amplification. Blood **95**, 1758-1766

28 Wong, K. K. (2007) HKI-272 in Non Small Cell Lung Cancer. Clin.Cancer Res. **13**, 4593s-4596s

29 Azam, M., Nardi, V., Shakespeare, W. C., Metcalf, C. A., III, Bohacek, R. S., Wang, Y., Sundaramoorthi, R., Sliz, P., Veach, D. R., Bornmann, W. G., Clarkson, B., Dalgarno, D. C., Sawyer, T. K. and Daley, G. Q. (2006) Activity of dual SRC-ABL inhibitors highlights the role of BCR/ABL kinase dynamics in drug resistance. Proc.Natl.Acad.Sci.U S A **103**, 9244-9249

30 Shah, N. P., Skaggs, B. J., Branford, S., Hughes, T. P., Nicoll, J. M., Paquette, R. L. and Sawyers, C. L. (2007) Sequential ABL kinase inhibitor therapy selects for compound drug-resistant BCR-ABL mutations with altered oncogenic potency. J.Clin.Invest. **117**, 2562-2569

31 Cortes, J., Jabbour, E., Kantarjian, H., Yin, C. C., Shan, J., O'Brien, S., Garcia-Manero, G., Giles, F., Breeden, M., Reeves, N., Wierda, W. G. and Jones, D. (2007) Dynamics of BCR-ABL kinase domain mutations in chronic myeloid leukemia after sequential treatment with multiple tyrosine kinase inhibitors. Blood **110**, 4005-4011

32 Khorashad, J. S., Milojkovic, D., Mehta, P., Anand, M., Ghorashian, S., Reid, A. G., de, M., V, Babb, A., de Lavallade, H., Olavarria, E., Marin, D., Goldman, J. M., Apperley, J. F. and Kaeda, J. S. (2008) In vivo kinetics of kinase domain mutations in CML patients treated with dasatinib after failing imatinib. Blood **111**, 2378-2381

Table 1. IC_{50} values (μM) of Ba/F3 cell lines expressing ErbB family members.

Inhibitors	Ba/F3/EGFR	Ba/F3/EGFR-L858R	Ba/F3/EGFR+ ErbB2	Ba/F3/ErbB2
Erlotinib	0.47	0.03	0.26	ND*
Lapatinib	2.0	1.7	0.56	0.05
CI-1033	$7.6X10^{-3}$	$7.5\ X10^{-4}$	$7.2X10^{-3}$	$6.5X10^{-3}$

Cells were plated in triplicate at 1 $x10^5$ cells per well and incubated with escalating concentrations of erlotinib (0-10 μM), lapatinib (0-5 μM) and CI-1033 (0-3 μM) for 48 hours. Cells expressing EGFR-L858R were exposed to lower concentrations of erlotinib (0-3 μM) and CI-1033 (0-0.3 μM). Proliferation was measured using the MTS-based cell viability assay. Growth curves and IC_{50} values were generated using Origin 7.5 software. All IC_{50} values are means of at least three independent experiments. * ND – not determined.

Table 2. IC_{50} (μM) and fold change of EGFR mutants.

Mutation	Screen[1]	Erlotinib	Lapatinib	CI-1033
wt		0.47 (X1)	2.13 (X1)	0.0076 (X1)
L718A	E, L	2.25 (X4.8)	>5 (>2.3)	0.022 (X2.9)
E762V[2]	E	-	-	-
M766T	E, C	2.15 (X4.6)	1.40 (X0.7)	0.059 (X7.8)
V769L	E, L	1.10 (X2.3)	>5 (>2.3)	0.0087 (X1.1)
T790M	E, L, C	>10 (>21)	>5 (>2.3)	0.082 (X10.8)
G796R	E, C	5.35 (X11.4)	>5 (>2.3)	0.77 (X101.3)
C797S	C	0.42 (X0.9)	4.04 (>1.9)	1.30 (X171.1)
K852T	E	2.05 (X4.4)	2.80 (X1.3)	0.013 (X1.7)
T854A	E, L	1.90 (X4)	>5 (>2.3)	0.027 (X3.6)

The sensitivity of Ba/F3 cells transduced with indicated EGFR mutants to EGFR inhibitors was determined by MTS assay. $1x\ 10^5$ cells per well in triplicate were incubated with escalating concentrations of erlotinib (0-10 μM), lapatinib (0-5 μM) and CI-1033 (0-3 μM) for 48h. Proliferation was measured using the MTS-based cell viability assay. Growth curves and IC_{50} values (μM) were generated using Origin 7.5 software. All values are means of at least two independent experiments. Fold change in IC_{50} values compared to wild-type (wt) are indicated in parenthesis. [1] E-erlotinib, L-lapatinib, C-CI-1033. [2] Cells not viable.

Table 3. IC_{50} (μM) and fold change of EGFR-L858R mutations.

Mutation	Screen[1]	Erlotinib	Lapatinib	CI-1033
L858R		0.030 (X1)	1.66 (X1)	0.00075 (X1)
L858R + L718A	E, L	0.52 (X17.3)	>5 (>3)	0.0084 (X11.2)
L858R + M766T[2]	E, C	0.15 (X5)	0.11 (X0.07)	0.0034 (X4.5)
L858R + T790M	E, L, C	>10 (>333)	>5 (>3)	0.022 (X29.3)
L858R + G796R[3]	E, C	-	-	-
L858R + C797S	C	0.040 (X1.3)	1.22 (X0.7)	0.17 (X226.7)
L858R + T854A	E, L	0.10 (X3.3)	3.80 (X2.3)	0.005 (X6.7)
L858R+T790M+ C797S	-	>10 (>333)	>5 (>3)	>3 (>4000)

Cells expressing EGFR-L858R proteins with indicated resistance mutations were incubated with increasing concentrations of erlotinib (0-10 μM), lapatinib (0-5 μM) and CI-1033 (0-3 μM) for 48h. EGFR-L858R cells were treated with erlotinib at 0-3 μM, lapatinib at 0-5 μM and CI-1033 at 0-0.3μM for 48h. Proliferation was measured and IC_{50} values (μM) were generated as described in Table 1. All values are means of at least two independent experiments. Fold change in IC_{50} values compared to L858R are indicated in parenthesis. [1] E-erlotinib, L-lapatinib, C-CI-1033. [2] Cell viability was impaired. [3] Cells were non-viable.

Table 4. IC_{50} (μM) and fold change for EGFR mutations in the presence of ErbB2.

Mutation	Screen[1]	Erlotinib	Lapatinib	CI-1033
wt		0.27 (X1)	0.56 (X1)	0.0072 (X1)
E762V	E	0.54 (X2)	0.17 (X0.3)	0.010 (X1.4)
V769L	E	0.84 (X3.1)	3.15 (X5.6)	0.018 (X2.5)
H773L	L	0.87 (X3.2)	>5 (>8.9)	0.017 (X2.4)
R776P	L	1.16 (X4.3)	>5 (>8.9)	0.029 (X4.0)
L777Q	L, E	1.57 (X5.8)	>5 (>8.9)	0.035 (X4.9)
L788V	L	0.59 (X2.2)	>5 (>8.9)	0.011 (X1.5)
K852T	E	2.1 (X7.8)	2.1 (X3.75)	0.039 (X5.4)
T854A	E, L	1.32 (X4.9)	>5 (>8.9)	0.027 (X3.8)

EGFR mutants were expressed in the presence of ErbB2 and their sensitivity to drugs was assessed by MTS assay as described previously. IC_{50} values (μM) and fold change in IC_{50} compared to wild-type (wt) are indicated. [1] E-erlotinib, L-lapatinib, C-CI-1033.

Titles and legends to figures

Figure 1. Chemical structures of ErbB family tyrosine kinase inhibitors. The reported selectivity profile versus the ErbB family members is indicated in parenthesis.

Figure 2. Activation of EGFR or ErbB2 leads to IL-3-independent growth of Ba/F3 cells. (**a**) Ba/F3 cell lines maintained in the presence of IL-3 were analysed by immunoblotting with anti-myc and anti-phospho-Y1092-EGFR antibodies. (**b**) Cells maintained in medium plus or minus 20 ng/ml EGF were assessed for their EGFR phosphorylation status by immunoblotting with anti-phospho-Y1092-EGFR and anti-myc antibodies. (**c**) Ba/F3 cells co-expressing EGFR and ErbB2 were analysed for phosphorylation of ErbB2 by immunoblotting with anti-phospho-Tyr1248-ErbB2 and anti-myc antibodies. (**d**) Ba/F3/ErbB2 cells were maintained in IL-3-free medium supplemented with 10 ng/ml heregulin. ErbB2 was immunoprecipitated via the myc tag. ErbB2 phosphorylation in total lysates and immunoprecipitates was analysed by probing with anti-phospho-Y1248-ErbB2 antibody. (**e**) Ba/F3 cells expressing ErbB family members were maintained in the presence or absence of EGF or heregulin. 5x 10^4 cells were plated in triplicate and cell number was assessed every 24h for 96h. Data points represent the mean of three replicate wells from three independent experiments.

Figure 3. Identification and mapping of key resistance mutations to structural models of EGFR complexed with erlotinib, lapatinib and 13-JAB. (**a**) Resistance mutations identified in erlotinib, lapatinib and CI-1033 screens in the presence or absence of ErbB2. Red shading represents observed mutants that directly contact ligand, blue – non-contact mutants and grey – clinically observed mutations. * Identified in conjunction with T790M. (**b-d**) Key resistance mutations mapped onto the (**b**) EGFR-erlotinib, (**c**) EGFR-lapatinib or (**d**) EGFR-13-JAB crystal structure. The EGFR structure is represented as a ribbon that traces the amino-acid backbone of the protein. The glycine-rich loop (p-loop) is shown in green, the hinge region is yellow, the gatekeeper residue is orange, the C-helix is red and the activation loop is maroon. Mutated amino acids and their side-chains are labeled on each diagram. Each diagram contains mutations detected in screens that were performed in the presence or absence of ErbB2.

Figure 4. Phosphorylation of EGFR mutants following exposure to erlotinib, lapatinib and CI-1033. All cell lines were treated with increasing concentrations of indicated inhibitors for 2h, cell lysates prepared and analysed for EGFR phosphorylation by probing with anti-phospho-EGFR-Y1092 and anti-myc antibodies. (**a**) Ba/F3 cells expressing EGFR-L858R or EGFR-L858R-T790M or EGFR-L858R-C797S were treated with the indicated concentrations of erlotinib or CI-1033 and the phosphorylation status of EGFR was analysed by immunoblotting. (**b**) The extent of EGFR Y1092 phosphorylation following exposure to increasing concentrations of lapatinib was assessed in Ba/F3 cells co-expressing ErbB2 with wild type EGFR, EGFR-L788V or EGFR-V769L.

Figure 5. Combinations of CI-1033 and erlotinib increase the degree of selective pressure. 2.5 x10^6 Ba/F3 cells were infected with the EGFR mutation library and plated in soft agar in the presence of 20 ng/ml EGF and differing concentrations of

erlotinib and CI-1033. The total number of drug resistant colonies was counted after two weeks growth.

Figure 1.

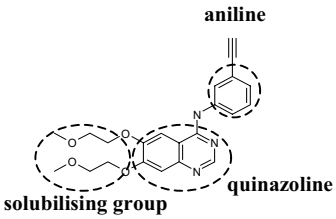

Erlotinib
(EGFR)

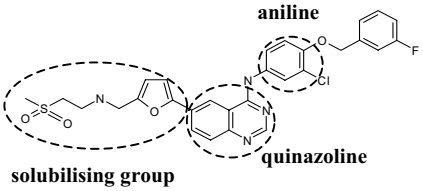

Lapatinib
(EGFR/ ErbB2)

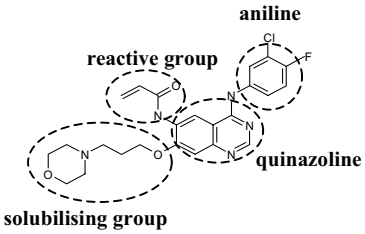

CI-1033
(EGFR/ErbB2/ErbB4)

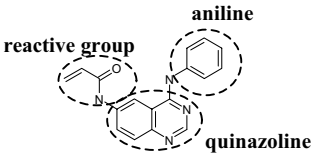

13-JAB
(EGFR)

Biochemical Journal Immediate Publication. Published on 30 Jun 2008 as manuscript BJ20080728

Figure 2.

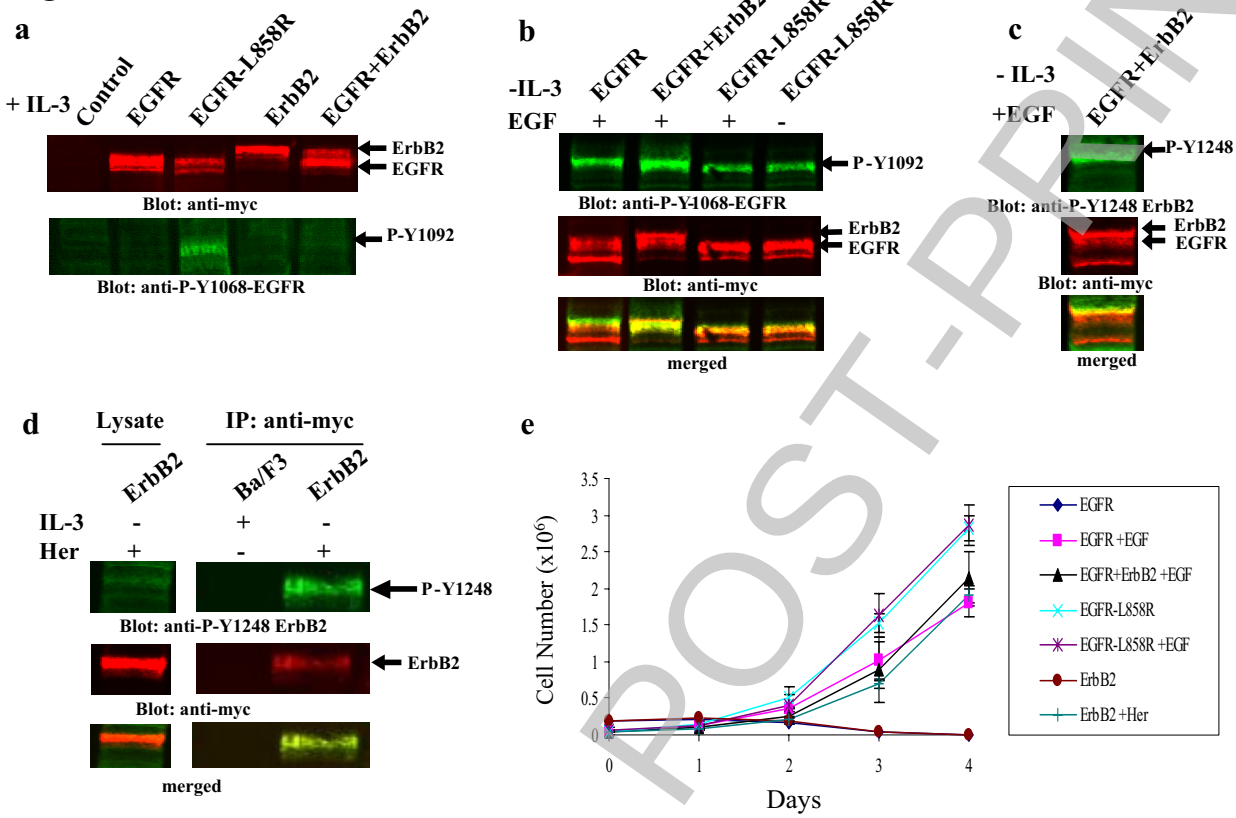

Biochemical Journal Immediate Publication. Published on 30 Jun 2008 as manuscript BJ20080728

Figure 3.

a

	Mutation	Erlotinib		Lapatinib		CI-1033	
			ErbB2		ErbB2		ErbB2
P-loop	L655P						
	M688V						
	E711D						
	E709G						
	L716I						
	L718Q						
	V742A						
	A743S						
	I744F						
C-helix	L747S						
	A750V						
	D761Y*						
	E762V						
	E762G						
	M766T						
	M766V						
	V769L						
	D770Y						
Selectivity pocket	H773L						
	C775F						
	R776P						
	L777M						
	L777Q						
	L778M						
	C781F						
	L788V						
	L788I						
Gatekeeper Hinge	T790M						
	P794L						
Solvent channel	G796D						
	G796R						
	G796C						
	C797S						
	C797G						
Activation loop	G810D						
	N816K						
	V845L						
	V845M						
	T847A						
	K852T						
	K852E						
	T854A						
	T854S						
	A859D						
	K860T						
	G863S						
	V876L						
	R889S						
	L907M						
	I965N						

b

Key mutations induced by erlotinib

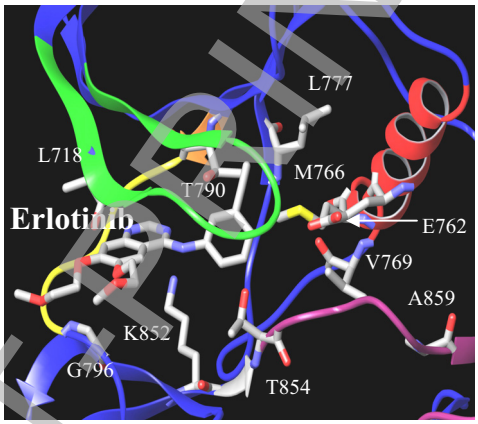

c

Key mutations induced by lapatinib

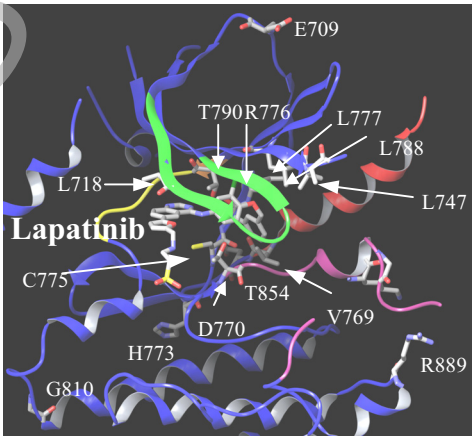

d

Key mutations induced by CI-1033

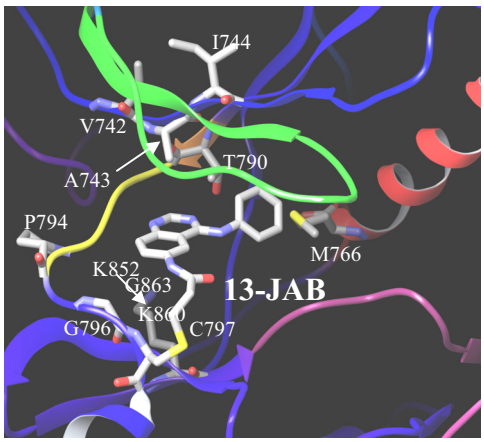

Biochemical Journal Immediate Publication. Published on 30 Jun 2008 as manuscript BJ20080728

Figure 4.

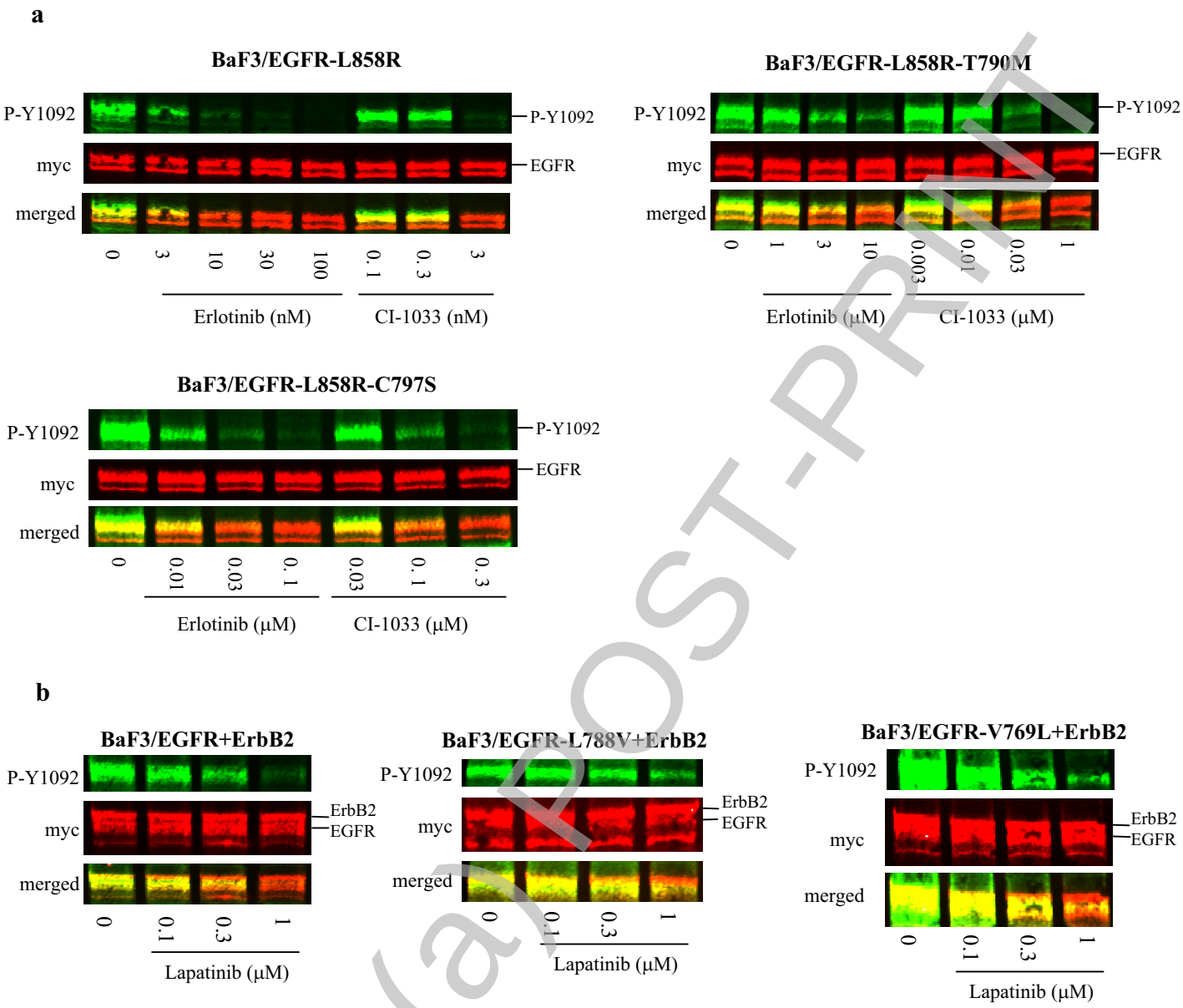

Figure 5.

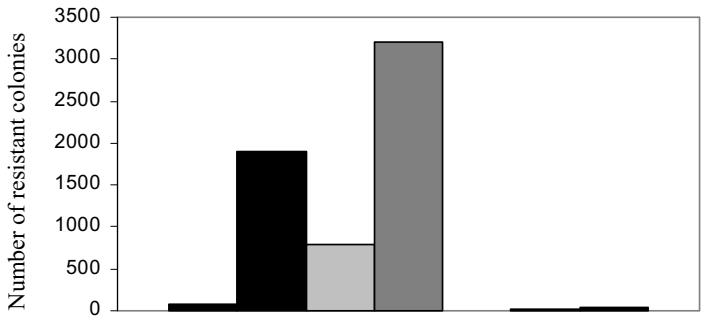

Erlotinib (μM)	2	1	-	-	2	2	1
CI-1033 (nM)	-	-	50	25	50	25	25
Colony number	76	1900	800	3200	8	20	34